Multi-frequency SuperDARN radar observations of the modulated ionosphere by high-power radio-waves at EISCAT

A. Mahmoudian [a,*], T.K. Yeoman [b], A. Senior [c], M. J Kosch [d,e,f], W.A. Scales [g], X. Shi [g], M. Ruohoniemi [g], M.T. Rietveld [h,i]

[a] *Institute of Geophysics, University of Tehran, Iran*
[b] *Department of Physics and Astronomy, University of Leicester, Leicester, UK*
[c] *Independent Researcher, Lancaster, UK*
[d] *Department of Physics, Lancaster University, Lancaster, UK*
[e] *South African National Space Agency (SANSA), Hermanus, South Africa*
[f] *Dept. of Physics and Astronomy, University of the Western Cape, Bellville, South Africa*
[g] *Bradley Department of Electrical and Computer Engineering, Virginia Tech, USA*
[h] *EISCAT Scientific Association, Ramfjordmoen, Norway*
[i] *Department of Physics and Technology, University of Tromsø-The Arctic University of Norway, Tromsø, Norway*

Abstract

This paper presents the first joint observations of multi-frequency SuperDARN (Super Dual Auroral Radar Network) radar of the heated ionosphere by high-power high-frequency (HF) ground-based radio-waves along with the stimulated electromagnetic emissions (SEE) measurements. The unique heating experiment design at EISCAT (The European Incoherent Scatter Scientific Association) including fine frequency stepping through the fourth electron gyro-frequency ($4f_{ce}$) provided the opportunity to directly determine the plasma waves responsible for SuperDARN radar echoes. Past experiments using a unique Kodiak SuperDARN receiver in Alaska with capability of data recording over a large bandwidth of frequencies different from the radar transmission frequency was able to detect some radar echoes due to pump-excited plasma waves. However, a precise characterization of these waves could not be reached in the past. Comparison of the behavior of the SEE data measured on the ground besides the multi-frequency SuperDARN observations above the heated ionosphere at EISCAT has shown a good correlation with the characteristics of upper-hybrid (UH)/electron Bernstein (EB) waves excited through parametric decay instability. The ray tracing model based on the EISCAT dynasonde data of the background ionospheric parameters has been used in order to determine the natural ionospheric effects on the propagation path of 9.9 MHz, 13.2 MHz, and 16.6 MHz signals associated with SuperDARN radar. By providing a more direct connection between SuperDARN echoes and the associated SEE measurements, this new technique potentially provides more quantitative characterization of plasma waves generated during ionospheric heating.

Keywords: Ionospheric heating; SuperDARN; Plasma waves; Upper hybrid; Ray tracing

1. Introduction

The excited SEEs (Stimulated Electromagnetic Emissions) within 1–100 kHz (known as wideband SEE or WSEE) of the HF pump radio-waves have been investigated in detail over the past three decades (Leyser, 2001). The recent studies have also revealed new unique features within 1 kHz of the HF pump field, which is known as narrowband SEE (NSEE) features (Norin et al., 2008; Bernhardt et al., 2009, 2010, 2011; Bordikar et al., 2013, 2014; Fu et al., 2013, 2015; Mahmoudian et al., 2013a,b,

* Corresponding author.
E-mail address: a.mahmoudian@ut.ac.ir (A. Mahmoudian).

2014a,b, 2016, 2019a,b; Yellu et al., 2018a,b, 2019). The recent works have proved the capability of SEE measurements in studying the excited plasma waves as well as the plasma related phenomena such as wave-particle interaction and non linear saturation, in the heated ionosphere. The SEE observations in many ways are much simpler than other plasma diagnostic techniques that require an active sources such as radar. While the early SEE measurements were not able to provide direct information regarding the electrostatic (ES) waves excited in the modified ionospheric plasma, recent advances in joint observations of SEE with radars as well as optical techniques has shown the great potential of this technique (Mahmoudian et al., 2013a).

Hughes et al. (2003, 2004) conducted the first experiment using the unique feature of Kodiak SuperDARN radar with the receiver capability of 1.5 kHz to ~1.2 MHz frequency bandwidths. The receiver could be tuned at a frequency different from the radar transmission frequency. The backscattered signal Kodiak radar spec- trum measured during HF pump heating was character- ized as enhanced radar echoes with zero frequency offset corresponding to field aligned irregularities (FAI) and a strong enhanced SuperDARN backscattered signal at the radar transmission frequency (f_r) plus the HAARP
HF frequency (f_H). High power radio waves strongly excite small-scale field-aligned plasma density irregularities (FAIs) where the pump wave frequency is close to the local upper hybrid frequency (e.g. Robinson, 1989 and references therein). These density irregularities are elongated in the direction of the geomagnetic field. Irregularities with scale sizes of a 10–20 m perpendicular to the magnetic field, depending on the radar transmit frequency, will coherently backscatter radar signals through Bragg scatter when the radio wave *k* vector is close to orthogonal to the magnetic field vector, *B*. The Super-DARN echo enhancements observed by Kodiak radar were attributed to the generated UH waves (Hughes et al., 2003). Two enhanced spectra peaks were also observed at ±85 and ±108 kHz with respect to $f_r + f_H$, which are believed to indicate the presence of additional ES fluctuations at those frequencies. The subsequent work by Hughes et al. (2004) focused on the wider range of the frequency range from ~55 kHz below to ~6.5 MHz above the f_r in order to determine the artificial stimulation of fluctuations perpendicular to B (presence of ES waves). They concluded that the several enhancements to the HF backscatter radar spectrum was observed dur- ing this experiment may indicate the excitation of electron Bernstein modes by the HF heater. While these two stud- ies are the sole work on this topic and incorporated a unique experimental design, no definite conclusion were made in regards to the ES plasma waves effects in the SuperDARN radar spectrum.

Another recent multi-frequency SuperDARN observation during X-mode ionospheric heating at EISCAT was reported by Blagoveshchenskaya et al. (2011). According to this work, the first excitation of FAI using X-mode HF pump wave is observed. While the generation of the X-mode Artificial FAIs (AFAIs) observed by SuperDARN radar was attributed to the short wavelength (upper-hybrid and electron Bernstein waves) plasma oscillations (Vas'kov and Ryabova, 1998), no clear physical evidence was reported in this study.

The main purpose of this manuscript is to take advantage of the heating experiment conducted at EISCAT along with the ray tracing results, three frequency SuperDARN observations, and SEE measurements in order to provide a direct characterization of ES plasma waves in Super- DARN data. The paper is organized as follow. The experimental set up is provided in Sections 2. The ray tracing calculations associated with the three SuperDARN frequencies are provided. The comparison of multi- frequency SuperDARN echoes with the ray tracing results obtained by real ionospheric parameters through EISCAT dynasonde data along with the ground SEE measurements and corresponding theories are provided. At the end, a summary of the correlation between different measurement techniques and the possible plasma waves responsible for the observations are provided.

2. Experimental setup

The data presented in this paper were obtained during a 2012 research campaign at the EISCAT HF facility (69.59 N, 19.21 E) located in Norway. The experiment on 2012-02-23 was designed to sweep the HF pump frequency around the fourth electron gyro-harmonic ($4f_{ce}$) (Mahmoudian et al., 2019a). The heating cycle of 30 min with 18 min ''on" period and 12 min ''off" period are considered. The experiment was repeated 4 times from 15:30 UT to 17:30 UT. The heating cycle included frequency steps from 5.3 to 5.6 MHz with an initial 130 s dwell time and 96 steps of 3.125 kHz each 10 s long. The total duration of the 18 min cycle was 1080 s. The gyro frequency near the reflection altitude was on the order of 1.35 MHz and the fourth harmonic lied near 5.4 MHz. The transmitter power was in the range 824–880 kW, and the antenna gain varies with frequency so that the effective radiated power was between 318 and 458 MW, assuming perfect ground conductivity. The beam direction was between 12 and 13 degrees south, very close to the magnetic field direction. It's noteworthy that a fifth heater cycle between 17:30 to 18:00 UT due to weaker signatures of SuperDARN echoes as well as SEE spectral lines is not included here.

3. Experimental observations

3.1. Ray tracing calculations

In order to characterize the signature of the generated plasma waves in the SuperDARN echo, the ray tracing plots associated with each heating cycle is provided. The code used in this paper was developed by Jones and

Stephenson (1975) with the orthogonality condition obtained from the IGRF. The ray path for three SuperDARN transmission frequencies is obtained using the EISCAT dynasonde data including the critical frequencies, heights and scale heights of the E and F layers. According to the dynasonde data a sporadic-E layer was present in the first heating cycle with a maximum plasma frequency of 1.3 MHz around 130 km, and a scale height of 16.4 km. No sporadic-E layer is observed in the subsequent heating cycles. The Table 1 demonstrates the α–Chapman ionospheric layer parameters used in the raytracing simulation.

The contours in Fig. 1 show the orthogonality condition between the radar k vector and the magnetic field, with the red color corresponding to the orthogonal path. The solid tilted line at a ground range of 800 km denotes the location of EISCAT HF facilities in Tromso, Norway and the direction of the associated magnetic field line. According to the ray tracing results, the most affected SuperDARN radar signal by the natural ionospheric plasma is the 10 MHz transmission frequency. As mentioned before the background ionospheric plasma parameters are imported into the model from the EISCAT dynasonde observations. The 10 MHz SuperDARN ray follows the earth-ionosphere reflection channel after being reflected by the natural ionospheric plasma. Therefore, the effect of artificial ionospheric irregularities excited through high-power radio-wave transmission using the EISCAT HF facility on 10 MHz SuperDARN signal is not prominent. As the SuperDARN transmission frequency increases to ~13 MHz and 16.6 MHz, the backscattered signal by the background ionospheric plasma reduces. This provides the opportunity to probe the artificial irregularities excited in the ionosphere and examine the plasma waves participating in the physical processes that results in the generation of such artificial turbulence.

As can be seen in Fig. 1, the orthogonality condition in the ionosphere above Tromso shown with bright colors of red and orange corresponding to angles smaller than 4 degrees with respect to the background magnetic field line. The range of excited FAI observed at each radar echo is consistent (Fig. 1) with the spatial distribution of FAI at the associated radar wavelength covered range orthogonal to B_0 and at the interaction region above the EISCAT heater. Specifically, according to Fig. 1, the spatial distance that the 10 MHz ray propagated in the heated region perpendicular to B_0 is much shorter than 13.2 MHz and 16.6 MHz, respectively. This manifest itself in the SuperDARN observations shown in Fig. 2. As can be seen in Fig. 2, the spatial expansion of radar echoes is in the range ~870–930 km, 870–970 km, 870–1050 km for 10, 13.2 and 16.6 MHz, respectively. Therefore, there is clear correlation between the spatial range orthogonal to B_0 ~60 km, 100 km, and 180 km corresponding to 10 MHz, 13.2 MHz, and 16.6 MHz) with the range estimated based on ray tracing calculations presented in Fig. 1. The intensity of radar echoes is also consistent with the number of rays passing through the heated region and perpendicular to B_0. According to Fig. 1, the number of ray paths passing through the heated region above EISCAT HF facility is much higher at 16.6 MHz than 10 MHz. Therefore, a general pattern of stronger radar echoes is expected at the 16.6 MHz SuperDARN signal mostly due to reflection by the generated artificial field aligned irregularities (FAI) and the corresponding plasma waves. This is also consistent with experimental SuperDARN observations presented in Fig. 2 that will be discussed shortly. The ray paths associated with the 10 MHz signal predicts stronger echoes for the 2 and 4 heating cycle (starting at 16:00 UT and 16:30 UT). The ray paths associated with 10 MHz in Fig. 1a–d predicts the ground scatter. A close comparison of the ray tracing results show that loss of backscatter is due to no FAI (excited UH/EB wave) on the signal path as the radar beam is no longer refracted enough to become orthogonal to the magnetic field in the heated volume for 10 MHz signal. In other words, the denser selection rays should sample the volume of ionosphere directly over the heating facility to produce the maximum effect, and this depends on frequency. It should also be noted that the majority of south direction rays clearly do not achieve orthogonality in the ray trace, which implies little or no backscatter but the data does show backscatter.

The least dependency of 10 MHz signal to artificial FAI is expected for the case shown in Fig. 1a (top panel). According to this figure due to the presence of sporadic E layer, most of the rays get reflected to the ground. This behavior validates the SuperDARN observations presented in Fig. 2b and d (second and fourth heating cycles), where the 10 MHz SuperDARN signal shows a good correlation with the artificial ionospheric irregularities. Such a signature is present in 13 and 16.6 MHz signals, which represent the similar pattern to the excited plasma waves responsible for FAI formation as will be

Table 1
α–Chapman ionospheric layer parameters used in the raytracing simulation in Fig. 1. The parameters FoF2, HmF2, yF2, FoE, HmE, and yE denote the maximum f_{pe}, associated height, and scale height for the F and E regions, respectively.

Date/Time	FoF2 (MHz)	HmF2 (km)	yF2 (km)	FoE (MHz)	HmE (km)	yE (km)
23 Feb 2012 15:30 UT	4.8	228	18	1.2	128	16.4
23 Feb 2012 16:00 UT	5.0	255	23	0	0	0
23 Feb 2012 16:30 UT	5.2	247	16	0	0	0
23 Feb 2012 17:00 UT	4.7	238	13	0	0	0

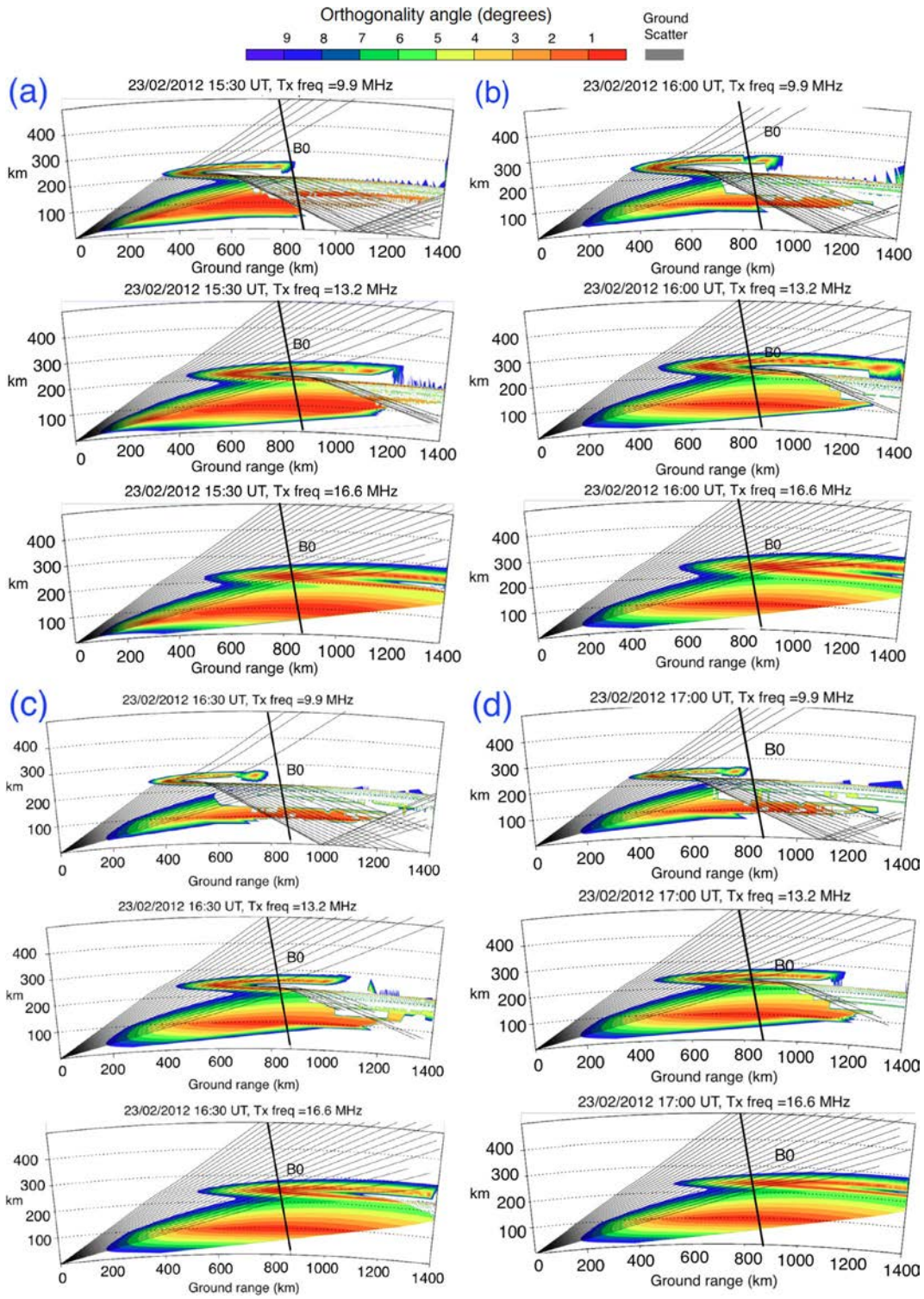

Fig. 1. Ray tracing results associated with three SuperDARN frequencies of 9.9 MHz, 13.2 MHz, and 16.6 MHz for 4 heating cycles starting at (a) 15:30 UT, (b) 16:00 UT, (c) 16:30 UT, () 17:00 UT. The ray paths are calculated using the ionospheric parameters obtained through EISCAT dynasonde observations of the critical frequencies, heights and scale heights of the E and F layers.

discussed in the following section. While the backscattered signal at 10 MHz is absent in Fig. 1a (first heating cycle), the third heating cycle shows a random scattering of 10 MHz signal (Fig. 2c). This will be discussed in more detail in the following sections.

3.2. SuperDARN observations

The modulated ionospheric F-region above the EISCAT HF heater was probed by CUTLASS Hankasalmi Super-DARN (HAN) radar located in Finland approximately

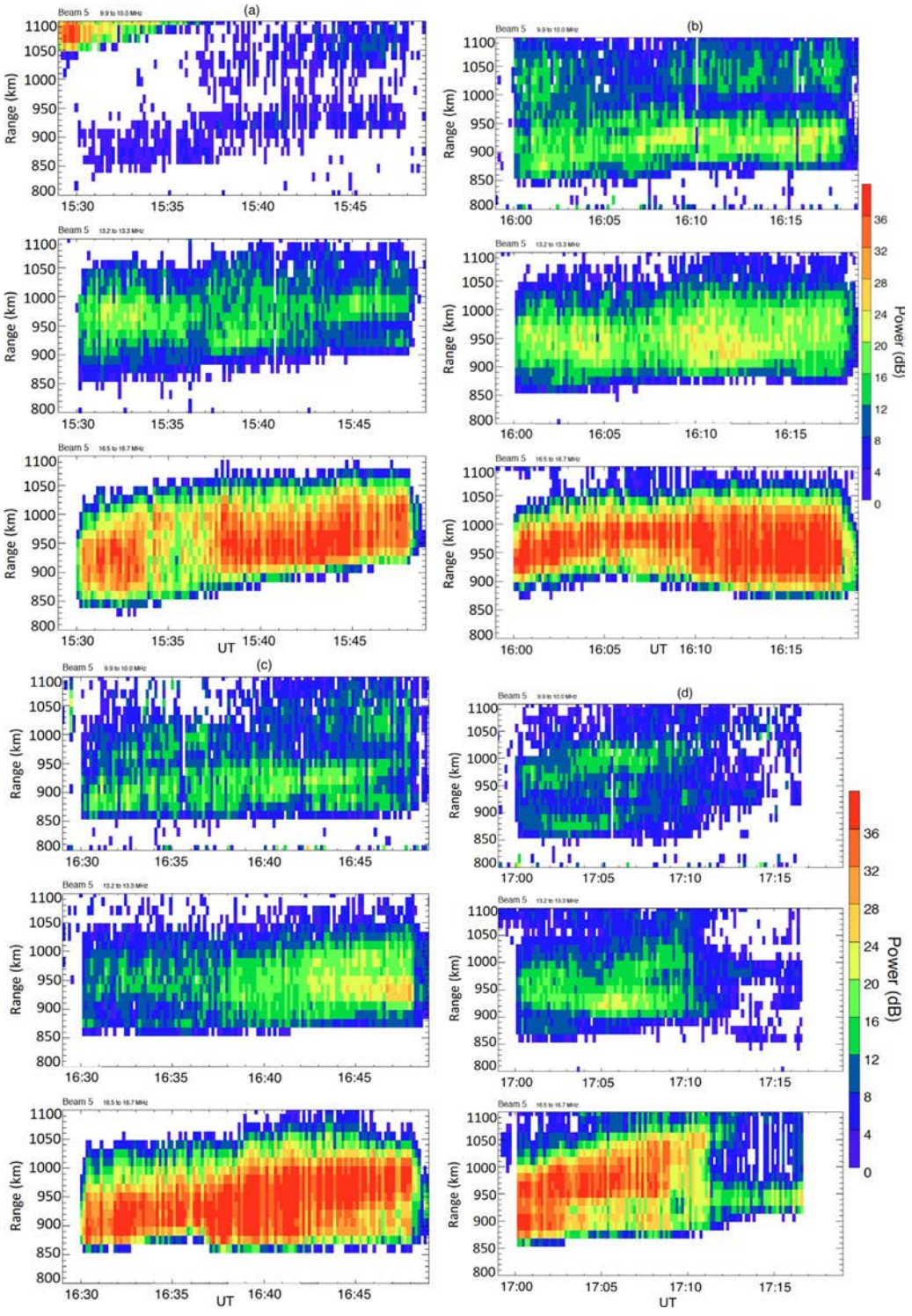

Fig. 2. SuperDARN observations during 18 min heating cycle associated with three SuperDARN frequencies of 9.9 MHz (top), 13.2 MHz (middle), and 16.6 MHz (bottom) for 4 heating cycles starting at (a) 15:30 UT, (b) 16:00 UT, (c) 16:30 UT, (d) 17:00 UT. The vertical and horizontal axis show the actual range from the radar. 1 min before and after the HF turn on and off, respectively, are shown as a reference for the formation of FAI during pump heating.

1000 km south of the Tromso heating facility (63ºN, 27ºE). The CUTLASS is a pair of HF coherent backscatter radars located in Finland and Iceland and forms part of the SuperDARN array (Lester et al., 2004). The beam 5 was utilized in this study among 16 independent radar beams that center on the Tromso HF heater. The radar beam is approximately 3.3º wide. The HAN SuperDARN radar data has temporal resolution of 1 s and 15 km range gates.

The mode plot shown in Fig. 2, has a lag to first range of 480 km and 15 km range gates, such that the gate 20 corresponds to a notional range of 780 km. A comparison of the SuperDARN observations in Fig. 2 and ray tracing results in Fig. 1 shows that the actual ground range of the scattered signal will be dependent on the ray group path. As shown in Fig. 2, the maximum path of the reflected ground scatter is rv1230 km.

Fig. 2a–d show the recorded HAN SuperDARN echoes at 10 MHz (top), 13.2 MHz (middle), and 16.6 MHz (bottom) associated with 4 heating cycles starting at 15:30 UT, 16:00 UT, 16:30 UT, and 17:00 UT, respectively. The SuperDARN frequencies are equivalent to AFAIs with the spatial size across the geomagnetic field of the order of $l_{\perp} \approx$ 15, 11, and 9 m, respectively. As can be seen in Fig. 2, the strongest SuperDARN echoes is observed at 16.6 MHz and throughout the whole heating cycle. A cut off in the radar echoes appears in the fourth heating cycle (Fig. 2d) around 17:12 UT (720 s after turn on) that is consistent with the ground observations of SEE as will be discussed subsequently. The weakest radar echoes are associated with radar frequency of 10 MHz. The 13.3 MHz signal shows a moderate reflection in comparison with 16.6 MHz and 10 MHz. This is in agreement with the ray tracing calculations presented in Fig. 1.

3.3. SEE measurements

Fig. 3 shows the WSEE measurements associated with four heating cycles. Several WSEE features including UM (upshifted maximum), DM (DM1 and DM2) (downshifted maximum), DP (downshifted peak), and BUM (broad upshifted maximum) are shown. As shown in Fig. 4, the generation mechanism of the DM line in the WSEE spectrum can be attributed to two different mechanisms (Leyser, 2001). In the first parametric decay instability, the EM HF pump wave decays to UH waves, which then decays to LH waves and an O-mode EM wave. In the proposed alternative approach, the EM pump wave decays to UH waves initially, then is converted to LH waves and electrostatic UH/EB waves. The latter generated waves will scatter off FAI and be converted to an EM waves propagating back to the ground (Leyser, 2001). These two concepts will be elaborated in the discussion section.

According to all cases shown in Fig. 3, the DM may weaken as the pump frequency passes through $4f_{ce}$, but it is mostly present throughout the heating cycle. The DM line is weaker for the pump frequencies below $4f_{ce}$, as the f_0 approaches $4f_{ce}$ the DM line starts to quench, then it becomes stronger for $f_0 > 4f_{ce}$. Such behavior can be seen in the simultaneous SuperDARN observations

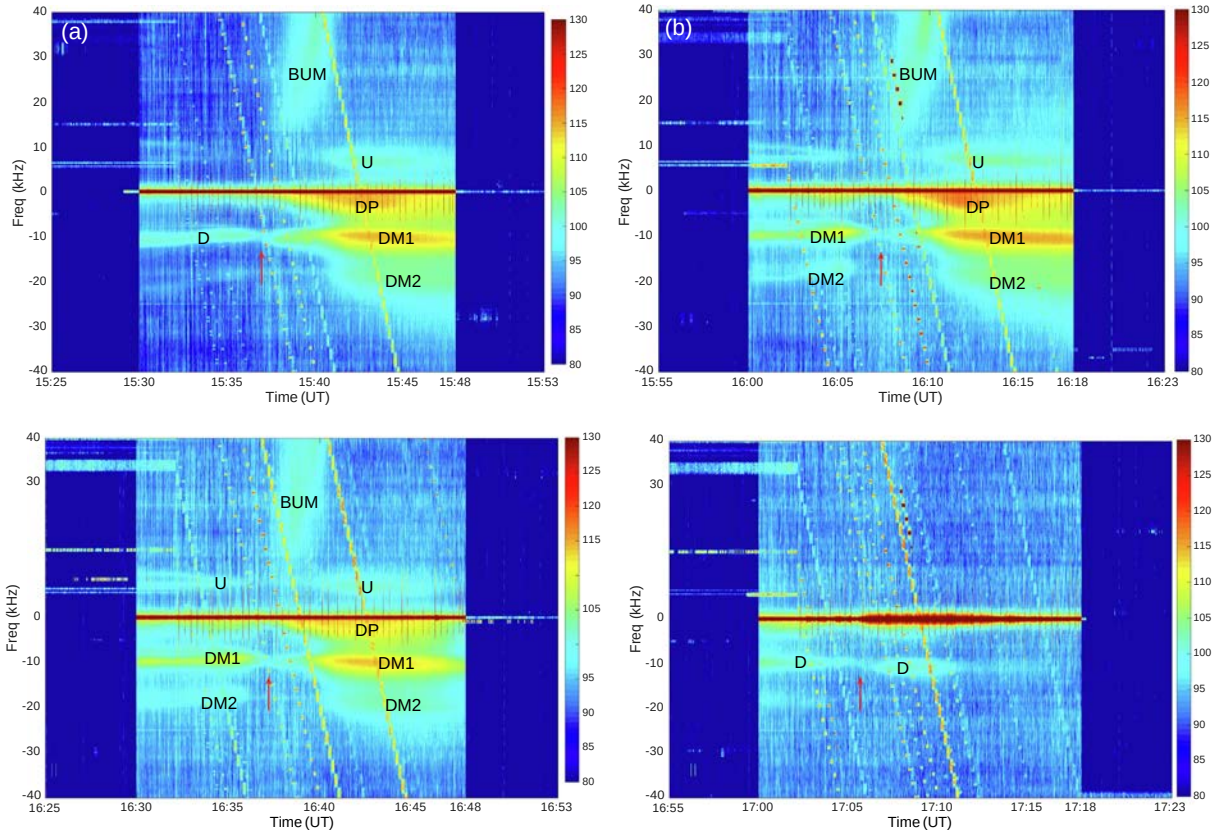

Fig. 3. Measured SEE spectral lines associated with the experiment conducted on Feb 23, 2012 for 4 heating cycles, broadband (WSEE) spectral lines including DM, DP, BUM, and UM in the frequency range of 40 kHz to +100 kHz of the pump frequency. The horizontal axis shows the time in seconds from the beginning of the heating cycles at 15:30 UT (a), 16:00 UT (b), 16:30 UT (c), and 17:00 UT (d), respectively. The red arrows denote the HF pump frequency crossing the local $4f_{ce}$ at the interaction altitude. The plotted frequency is the offset from the pump frequency.

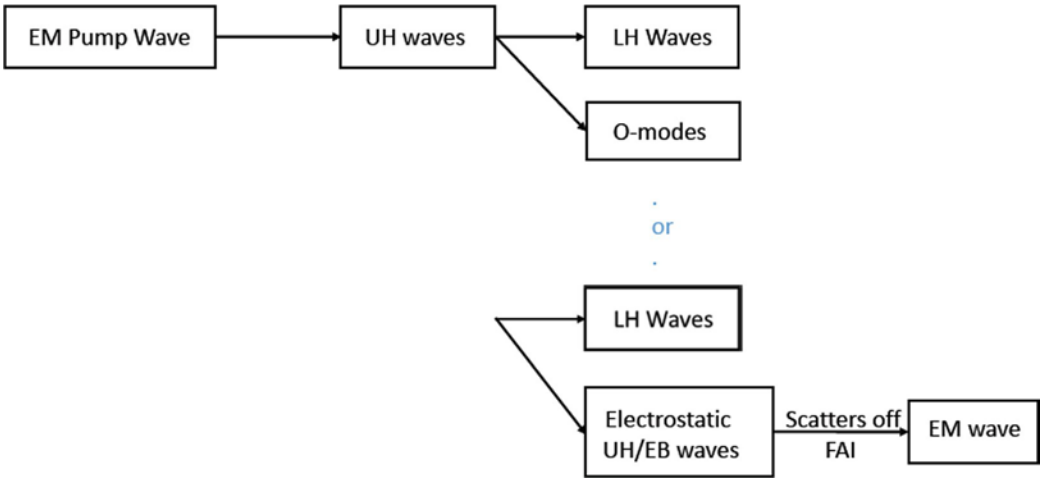

Fig. 4. The proposed parametric decay instability (PDI) responsible for the DM emission line including indirect and direct mode conversions involving UH/EB waves responsible for SuperDARN radar echoes.

as will be discussed in the following section. It should be noted that the behavior of BUM spectral line for HF pump frequency sweeping through 4fce and its correlation with the incoherent scatter radar (ISR) spectra features including enhanced-ion lines (EHIL) is studied in the recent paper by Mahmoudian et al. (2019a).

4. Discussion

The main purpose of this paper is to continue the previous work done by Hughes et al. (2003, 2004), where they studied the signature of induced plasma waves in the heated region above HAARP using the Kodiak SuperDARN radar. Specifically, they used the Kodiak radar spectrum at frequencies equal to the radar plus the heater frequencies ($f_r + f_H$) to observe any modulation effects with the pump frequency as well as spectrum side-bands due to possible modulation of radar signal with excited plasma waves. They provided evidence of the spectral enhancements and attributed that to perpendicularly propagating upper hybrid (UH) waves. Bernhardt et al. (1994) has demonstrated that this scatter process with enhanced FAI production with a second HF pump wave at an offset frequency. The UH waves are believed to exist near the UH resonance layer. While UH wave excitation is critical in ionospheric heating experiments, very few direct observations have indicated their presence in the heated volume. This paper tries to draw a connection between multi-frequency and simultaneous observations of SuperDARN echoes from the heated ionospheric region along with the ray tracing calculations as well as ground-based SEE measurements. According to ray tracing results, a strong correlation between the radar echoes and estimated rays passing through the heated region is observed. A clear double layer reflection of 10 MHz radar signal can be seen for cases b and d (Fig. 2). This is consistent with the prediction of ray tracing results that shows more escape of 10 MHz rays from the natural ionosphere (Fig. 1b, d). Moreover, the orthogonality condition of HAN SuperDARN beam 5 with the heated ionosphere above Tromso shows consistency with the predicted ray tracing results.

The DM line is excited near the double resonance layer where $\omega_0 = \omega_{UH} = n\Omega_{ce}$. In this expression the upper-hybrid frequency is $\omega_{UH} = \sqrt{\omega_{pe}^2 + \Omega_{ce}^2}$. The DM line is attributed to the nonlinear interaction of pump excited UH and LH waves. There are two important parameters that could affect the presence of the DM line. The plasma inhomogeneities as well as local variation of f_{ce} could destroy the double resonance condition over which the DM is excited. According to Leyser et al. (1994), the spatial region (height extension near double resonance altitude) is required for the PDI to develop and result in the generation of DM. Trapping of plasma waves in density depletion has been suggested to be an important mechanism for the generation of small-scale field-aligned striations. HF enhanced striations have been proposed to be due to the thermal OTSI (oscillating two stream instability) (Huang and Kuo, 1994). Such small-scale FAI are extended about 1 km along *B*, with a size of few meters perpendicular to *B* through thermal instabilities. The altitude range over which thermal OTSI can be excited reduces significantly as the pump frequency approaches nf_{ce}. The weakening of striations decreases the wave trapping which is consistent with the suppression of the DM line. It should be noted that a close comparison to Fig. 2, shows a small suppression of radar echoes at 16.6 MHz around 15:36 UT (Fig. 2a, bottom) and 17:05 UT (Fig. 2d). This is consistent with the proposed theory of small weakening of striations for $f_0 \sim 4f_{ce}$, which reduces plasma wave trapping and results in the suppression of DM line. The behavior of 13.3 MHz radar echoes in heating cycles b and c is well consistent with the behavior of DM line in the WSEE spectrum (Fig. 3b and c). Both cases represent a suppression of 13.3 MHz SuperDARN echoes as the pump frequency

swept through $4f_{ce}$. Moreover, a weaker pattern of radar echoes for $f_0 < 4f_{ce}$ in comparison with the $f_0 > 4f_{ce}$ is observed in Fig. 2b and c, which is in a close agreement with the time evolution of the DM line. The radar echoes disappear 17:12 UT (Fig. 2d) in all radar frequencies which is in agreement with the ground measurements of the excited WSEE DM emission lines. Also, the WSEE spectrum only shows the DM line for the case d. Such clear correlations could validate the presence of UH/EB waves in SuperDARN echoes.

Rao and Kaup (1992) suggested that the mode conversion of UH wave to LH wave (lower-hybrid) could explain the quenching DM line for $f_0 \sim nf_{ce}$. This process is proposed to happen within a few kHz of the nf_{ce} that is about 6 kHz for $f_0 \sim 4f_{ce}$. The behavior of SuperDARN echoes in case *d* that shows no clear signature of suppression for $f_0 \sim 4f_{ce}$ could be attributed to this mechanism.

5. Summary and conclusion

The previous work by Hughes et al. (2003) used a unique SuperDARN mode with receiving capabilities of bandwidth value from 1.5 kHz to 1.2 MHz as well as tunable receiver frequency independently from the transmitter frequency, which could show the connection between the SuperDARN echoes with UH wave signature excited during ionospheric HF pump heating. With a cautious conclusion, Hughes et al. (2004) reported spectral enhancements symmetrically distributed around offsets near electron gyro-harmonics that may therefore be signatures of Bernstein modes.

Considering the similar geometry of CUTLASS Hankasalmi SuperDARN radar with respect to the Tromso heating facility to the Kodiak radar observations with respect to the HAARP facility in Alaska, the present paper aims at the investigation of the electrostatic (ES) plasma waves excited during ionospheric heating at EISCAT. The main advantage of the experiment set up used here was to incorporate the multi-frequency SuperDARN observations rather than the spectral capability used in Alaska (Hughes et al., 2003, 2004), in order to characterize the presence of plasma waves responsible to the scattering of orthogonal radar signal in the interaction region. The radar echo enhancements result from interactions with UH waves propagating perpendicular to background magnetic field (B) rather than from interactions with Langmuir waves propagating nearly parallel to B. Therefore, the present study provides the first multi-frequency SuperDARN observations along with the ground SEE measurements, and ray tracing results during HF pump heating of the ionosphere with varying transmission frequency near $4f_{ce}$ in order to investigate the role of excited plasma waves in SuperDARN echoes. The first direct signature of the excited upper-hybrid (UH) and electron Bernstein (EB) waves in the SuperDARN observations has been reported using the comparison of the SEE spectral features including downshifted maximum (DM) as well as the ray tracing calculations. The ray tracing results verified that the observed behavior in three associated SuperDARN transmission frequencies is consistent with the SuperDARN echoes as well as the DM behavior during HF pump frequency variation near $4f_{ce}$. The higher radar frequencies at 13 MHz and 16.6 MHz are expected to show the modulation with the excited ionospheric irregularities (artificial FAI) as well as the generated plasma waves such as UH/EB waves. The CUTLASS SuperDARN echoes correlate well with the time evolution of DM emission line, which corresponds to the mode conversion of the HF pump wave to UH waves. This validates the previous results provided by Hughes et al. (2003, 2004) that SuperDARN echoes generated near UH resonance layer are mostly due to field aligned irregularities with fluctuations at different wavelengths perpendicular to background magnetic field and distributed periodically along the magnetic field line and representative of the excited UH/EB modes. The geometry of the observations based on the ray tracing calculations near the interaction region also validates this assumption. In summary, the observations presented in this paper are in favor of the first theory that explains the generation of the DM line as well as its weakening for f_0 close to $4f_{ce}$.

It should be noted that the previous work by Mahmoudian et al. (2019a) reported the first detailed study on the comparison of SEE spectral lines, including narrowband 1 kHz and wide-band 10 kHz, with the ISR spectral feature, mainly enhanced ion lines. Therefore, this companion paper aims to prove the great potential of ground-based observations of SEE in validating the physics of ionospheric heating experiments and the excited plasma waves and irregularities within modulated ionosphere. Such diagnostics can be used as a remote sensing tool in space plasma as well as a new measurement technique in the laboratory. In summary, the spectral scatter approach used by Hughes et al. (2003, 2004) is one of the greatest mysteries in the ionospheric modification science and should be repeated to observe the spectral content of the HF radar scatter. The addition of simultaneous SEE observations may be able to clear up this harmonic generation and frequency mixing process.

Acknowledgements

EISCAT is an international association supported by research organizations in China (CRIRP), Finland (SA), Japan (NIPR and STEL), Norway (NFR), Sweden (VR), and the United Kingdom (NERC).

References

Bernhardt, P.A., Wagner, L.S., Goldstein, J.A., Trakhtengerts, V.Yu., Ermakova, E.N., Rapoport, V.O., Komrakov, .P., Babichenko, A.M., 1994. Enhancement of stimulated electromagnetic emission during two frequency ionospheric heating experiments. Phys. Rev. Lett. 72, 2879–2882.

Bernhardt, P.A., Selcher, C.A., Lehmberg, R.H., Rodriguez, S., Thomason, J., McCarrick, M.J., Frazer, G., 2009. Determination of the

electron temperature in the modified ionosphere over HAARP using the HF pumped Stimulated Brillouin Scatter (SBS) emission lines. Ann. Geophys. 27, 4409–4427. https://doi.org/10.5194/angeo-27-4409-2009.

Bernhardt, P.A., Selcher, C.A., Lehmberg, R.H., Rodriguez, S.P., Thomason, J.F., Groves, K.M., McCarrick, M.J., Frazer, G.J., 2010. Stimulated Brillouin scatter in a magnetized ionospheric plasma. Phys. Rev. Lett. 104 (165), 004. https://doi.org/10.1103/PhysRevLett.104.165004.

Bernhardt, P.A., Selcher, C.A., Kowtha, S., 2011. Electron and ion Bernstein waves excited in the ionosphere by high power EM waves at the second harmonic of the electron cyclotron frequency. Geophys. Res. Lett. 38, L19107. https://doi.org/10.1029/2011GL049390.

Blagoveshchenskaya, N.F., Borisova, T.D., Yeoman, T.K., Rietveld, M. T., Ivanova, I.M., Baddeley, L.J., 2011. Artificial small-scale field-aligned irregularities in the high latitude F region of the ionosphere induced by an X-mode HF heater wave. Geophys. Res. Lett. 38, L08802. https://doi.org/10.1029/2011GL046724.

Bordikar, M.R., Scales, W.A., Samimi, A., Bernhardt, P.A., Briczinski, S., McCarrick, M.J., 2013. First observations of minority ion (H^+) structuring in stimulated radiation during second electron gyro-harmonic heating experiments. Geophys. Res. Lett. 40, 1479AS1483. https://doi.org/10.1002/grl.50327.

Bordikar, M.R., Scales, W.A., Mahmoudian, A., Kim, H., Bernhardt, P. A., Redmon, R., Samimi, A.R., Brizcinski, S., McCarrick, M.J., 2014. Impact of active geomagnetic conditions on stimulated radiation during ionospheric second electron gyroharmonic heating. J. Geophys. Res. Space Phys. 119. https://doi.org/10.1002/2013JA019367.

Fu, H., Scales, W.A., Bernhardt, P.A., Samimi, A., Mahmoudian, A., Briczinski, S.J., McCarrick, M.J., 2013. Stimulated Brillouin scatter and stimulated ion Bernstein scatter during electron gyroharmonic heating experiments. Radio Sci. 48, 607–616. https://doi.org/10.1002/2013RS005262.

Fu, H., Scales, W.A., Bernhardt, P.A., Briczinski, S.J., Kosch, M.J., Senior, A., Rietveld, M.T., Yeoman, T.K., Ruohoniemi, J.M., 2015. Stimulated Brillouin scattering during electron gyroharmonic heating at EISCAT. Ann. Geophys. 33, 983–990.

Huang, J., Kuo, S.P., 1994. Cyclotron harmonic effect on the thermal oscillating two-stream instability in the high latitude ionosphere. J. Geophys. Res. 99, 2173.

Hughes, J.M., Bristow, W.A., Parris, R.T., Lundell, E., 2003. Super-DARN observations of ionospheric heater – induced upper hybrid waves. Geophys. Res. Lett. 30 (24), 2276. https://doi.org/10.1029/2003GL018772.

Hughes, J.M., Bristow, W.A., Parris, R.T., 2004. SuperDARN observations of spectral enhancements excited during an ionospheric heating experiment. Geophys. Res. Lett. 31, 8.

Jones, R.M., Stephenson, J.J., 1975. A versatile three-dimensional ray tracing computer program for radio waves in the ionosphere. NASA STI/Recon Technical Report N 76 (25), 476.

Lester, M., Chapman, P.J., Cowley, S.W.H., Crooks, S.J., Davies, J.A., Hamadyk, P., McWilliams, K.A., Milan, S.E., Parsons, M.J., Payne, D.B., Thomas, E.C., Thornhill, J.D., Wade, N.M., Yeoman, T.K., Barnes, R.J., 2004. Stereo CUTLASS - a new capability for the SuperDARN HF radars. Ann. Geophys. 22, 459–473. https://doi.org/10.5194/angeo-22-459-2004.

Leyser, T.B., 2001. Stimulated electromagnetic emissions by high-frequency electromagnetic pumping of the ionospheric plasma. Space Sci. Rev. 98, 223–328.

Leyser, T.B., Thidé, B., Waldenvik, M., Veszelei, E., Frolov, V.L., Grach, S.M., Komrakov, G.P., 1994. Downshifted maximum features in stimulated electromagnetic emission spectra. J. Geophys. Res. 99 (A10), 19555–19568. https://doi.org/10.1029/94JA01399.

Mahmoudian, A., Scales, W.A., Bernhardt, P.A., Samimi, A., Kendall, E., Ruohoniemi, J.M., Isham, B., Vega-Cancel, O., Bordikar, M., 2013a. Ion gyro-harmonic structuring in the stimulated radiation spectrum and optical emissions during electron gyro-harmonic heating. J. Geophys. Res. Space Phys. 118, 1270–1287. https://doi.org/10.1002/jgra.50167.

Mahmoudian, A., Scales, W.A., Bernhardt, P.A., Fu, H., Briczinski, S.J., McCarrick, M.J., 2013b. Investigation of ionospheric stimulated Brillouin scatter generated at pump frequencies near electron gyro-harmonics. Radio Sci. 48, 685–697. https://doi.org/10.1002/2013RS005189.

Mahmoudian, A., Scales, W.A., Bernhardt, P.A., Isham, B., Kendall, E., Briczinski, S.J., Fuentes, N.E.B., Vega-Cancel, O., 2014a. Electron gyroharmonic effects on ionospheric stimulated Brillouin scatter. Geophys. Res. Lett. 41, 5710–5716. https://doi.org/10.1002/2014GL061050.

Mahmoudian, A., Scales, W.A., Bordikar, M.R., Samimi, A., Bernhardt, P.A., 2014b. Narrowband Stimulated Electromagnetic Emissions (SEE) Spectra: A New Ionospheric Diagnostic Technique, General Assembly and Scientific Symposium, URSI.

Mahmoudian, A., Scales, W.A., Watkins, B.J., Bernhardt, P.A., Isham, B., Vega-Cancel, O., Ruohoniemi, J.M., 2016. Investigation of third gyro-harmonic heating at HAARP using stimulated radio emissions and the MUIR and Kodiak radars. Adv. Space Res. 59 (1), 337–350. https://doi.org/10.1016/j.asr.2016.09.029.

Mahmoudian, A., Senior, A., Kosch, M.J., Scales, W.A., Rietveld, M.T., Isham, B., Shi, X., Ruohoniemi, M., 2019a. Investigation of incoherent scatter radar spectra features with stimulated electromagnetic emissions at EISCAT. Adv. Space Res. 64 (1), 159–170. https://doi.org/10.1016/j.asr.2019.03.028.

Mahmoudian, A., Nossa, E., Isham, B., Bernhardt, P.A., Briczinski, S.J., Sulzer, M., 2019b. NSEE yielding electron temperature measurements at the Arecibo Observatory. J. Geophys. Res.: Space Phys. 124, 3699–3708. https://doi.org/10.1029/2019JA026594.

Norin, L., Grach, S.M., Leyser, T.B., Thide, B., Sergeev, E.N., Berlin, M., 2008. Ionospheric plasma density irregularities measured by stimulated electromagnetic emission. J. Geophys. Res. 113, A09314. https://doi.org/10.1029/2008JA013338.

Rao, N.N., Kaup, D.J., 1992. Excitation of electron cyclotron harmonic waves in ionospheric modification experiments. J. Geophys. Res. 97, 6323–6341.

Robinson, T.R., 1989. The heating of the high latitude ionosphere by high power radio waves. Phys. Rep. 179, 79–209.

Vas'kov, V.V., Ryabova, N.A., 1998. Nonlinear resonance of plasma waves in the thermal irregularities of ionospheric plasma. Radiophys. Quantum Electron 41, 177–195. https://doi.org/10.1007/BF02676535.

Yellu, A.D., Scales, W.A., Mahmoudian, A., Siefring, C., Bernhardt, P. A., 2018a. Initial results of stimulated radiation measurements during the HAARP campaign of September 2017. Radiat. Eff. Defects Solids 173 (1–2), 66–72.

Yellu, A.D., Scales, W.A., Mahmoudian, A., Bernhardt, P.A., Siefring, C. L., McCarrick, M.J., 2018b. First observations of narrowband stimulated electromagnetic emissions at the pump frequency second harmonic during ionosphere interaction experiments. Geophys. Res. Lett. 45. https://doi.org/10.1029/2018GL078924.

Yellu, A.D., Scales, W.A., Mahmoudian, A., Bernhardt, P.A., Siefring, C. L., Briczinski, S., 2019. Pump power effects on second harmonic stimulated electromagnetic emissions during ionosphere heating. J. Geophys. Res.: Space Phys. 124. https://doi.org/10.1029/2019JA027282.